J Physiol 593.20 (2015) pp 4531–4548

The Journal of Physiology

Membrane potential governs calcium influx into microvascular endothelium: integral role for muscarinic receptor activation

Erik J. Behringer[1] and Steven S. Segal[1,2]

[1] *Department of Medical Pharmacology and Physiology, University of Missouri, Columbia, MO 65212, USA*
[2] *Dalton Cardiovascular Research Center, Columbia, MO 65211, USA*

Key points

- Endothelial function in resistance vessels entails Ca^{2+} and electrical signalling to promote vasodilatation and increase tissue blood flow. Whether membrane potential (V_m) governs intracellular calcium concentration ($[Ca^{2+}]_i$) of the endothelium remains controversial.
- $[Ca^{2+}]_i$ and V_m were evaluated simultaneously during intracellular current injection using intact endothelial tubes freshly isolated from mouse skeletal muscle resistance arteries.
- $[Ca^{2+}]_i$ did not change during hyperpolarization or depolarization under resting conditions. However in the presence of 100 nM ACh ($\sim EC_{50}$), $[Ca^{2+}]_i$ increased during hyperpolarization and decreased during depolarization. These responses required extracellular Ca^{2+} and were attenuated by half with genetic ablation of TRPV4 channels.
- In native microvascular endothelium, half-maximal stimulation of muscarinic receptors enables V_m to govern $[Ca^{2+}]_i$ by activating Ca^{2+}-permeable channels in the plasma membrane. This effect of V_m is absent at rest and can be masked during maximal receptor stimulation.

Abstract In resistance arteries, coupling a rise of intracellular calcium concentration ($[Ca^{2+}]_i$) to endothelial cell hyperpolarization underlies smooth muscle cell relaxation and vasodilatation, thereby increasing tissue blood flow and oxygen delivery. A controversy persists as to whether changes in membrane potential (V_m) alter endothelial cell $[Ca^{2+}]_i$. We tested the hypothesis that V_m governs $[Ca^{2+}]_i$ in endothelium of resistance arteries by performing Fura-2 photometry while recording and controlling V_m of intact endothelial tubes freshly isolated from superior epigastric arteries of C57BL/6 mice. Under resting conditions, $[Ca^{2+}]_i$ did not change when V_m shifted from baseline (~ -40 mV) via exposure to 10 μM NS309 (hyperpolarization to ~ -80 mV), via equilibration with 145 mM $[K^+]_o$ (depolarization to ~ -5 mV), or during intracellular current injection (± 0.5 to 5 nA, 20 s pulses) while V_m changed linearly between ~ -80 mV and $+10$ mV. In contrast, during the plateau (i.e. Ca^{2+} influx) phase of the $[Ca^{2+}]_i$ response to approximately half-maximal stimulation with 100 nM ACh ($\sim EC_{50}$), $[Ca^{2+}]_i$ increased as V_m hyperpolarized below -40 mV and decreased as V_m depolarized above -40 mV. The magnitude of $[Ca^{2+}]_i$ reduction during depolarizing current injections correlated with the amplitude of the plateau $[Ca^{2+}]_i$ response to ACh. The effect of hyperpolarization on $[Ca^{2+}]_i$ was abolished following removal of extracellular Ca^{2+}, was enhanced subtly by raising extracellular $[Ca^{2+}]$ from 2 mM to 10 mM and was reduced by half in endothelium of TRPV4$^{-/-}$ mice. Thus, during submaximal activation of muscarinic receptors, V_m can modulate Ca^{2+} entry through the plasma membrane in accord with the electrochemical driving force.

© 2015 The Authors. The Journal of Physiology © 2015 The Physiological Society

DOI: 10.1113/JP271102

(Resubmitted 12 June 2015; accepted after revision 3 August 2015; first published online 10 August 2015)
Corresponding author S. S. Segal: Department of Medical Pharmacology and Physiology, 1 Hospital Drive, MA415 Medical Science Building, University of Missouri, Columbia, MO 65212, USA. Email: segalss@health.missouri.edu

Abbreviations ACh, acetylcholine; BK_{Ca}, large-conductance Ca^{2+}-activated K^+ channel; $[Ca^{2+}]_i$, intracellular Ca^{2+} concentration; $[Ca^{2+}]_o$, extracellular Ca^{2+} concentration; EC, endothelial cell; EC_{50}, drug concentration giving half-maximal response; E_K, Nernst equilibrium potential for K^+; ER, endoplasmic reticulum; FCCP, carbonyl cyanide p-trifluoromethoxyphenylhydrazone; GSK101, GSK1016790A; GSK219, GSK2193874; ID, internal diameter; $[K^+]_o$, extracellular K^+ concentration; NO, nitric oxide; OD, outer diameter; PSS, physiological salt solution; SEA, superior epigastric artery; SK_{Ca}/IK_{Ca}, small- and intermediate-conductance Ca^{2+}-activated K^+ channels; SMC, smooth muscle cell; TRP, transient receptor potential; TRPV4, transient receptor potential vanilloid type 4 channel; $TRPV4^{-/-}$, TRPV4 knockout; V_m, membrane potential.

Introduction

A key role for the endothelium of resistance vessels entails the regulation of intracellular Ca^{2+} ($[Ca^{2+}]_i$) and membrane potential (V_m) to govern smooth muscle cell (SMC) relaxation, vasodilatation and tissue blood flow (Busse *et al.* 2002; Ledoux *et al.* 2006; Bagher & Segal, 2011; Garland *et al.* 2011). The activation of G_q protein-coupled muscarinic (M_3) receptors stimulates the production of inositol 1,4,5-trisphosphate and diacylglycerol. Through binding to its receptor on the endoplasmic reticulum (ER), inositol 1,4,5-trisphosphate evokes the release of Ca^{2+} from internal stores as reflected by the initial peak of the Ca^{2+} response (Himmel *et al.* 1993). In turn, emptying intracellular Ca^{2+} stores stimulates the activation of Ca^{2+} permeable channels in the plasma membrane (which include an array of transient receptor potential (TRP) channels; Yue *et al.* 2015) and the ensuing plateau phase of the $[Ca^{2+}]_i$ response (see Dora & Garland, 2013; Ruhle & Trebak, 2013 for details regarding the regulation Ca^{2+} influx). The rise in $[Ca^{2+}]_i$ activates small- and intermediate-conductance Ca^{2+}-activated K^+ channels (SK_{Ca}/IK_{Ca}) in the plasma membrane as reflected by endothelium-dependent hyperpolarization in response to muscarinic receptor stimulation. While the ensuing efflux of K^+ results in a more negative cell interior, it remains controversial as to whether hyperpolarization enhances Ca^{2+} entry into endothelial cells (ECs) by increasing its electrical driving force (Dora & Garland, 2013). With production of nitric oxide (NO) as a vasodilator also governed by a rise in $[Ca^{2+}]_i$ (Busse & Mulsch, 1990), the regulation of Ca^{2+} entry in the endothelium of resistance vessels is integral to the control of tissue blood flow and oxygen delivery.

The influx of Ca^{2+} is driven by an ∼20,000-fold concentration gradient from the extracellular fluid, electronegativity of the cell interior and the open probability of Ca^{2+}-permeable ion channels (Clapham, 2007). Previous endeavours to assess whether V_m impacts Ca^{2+} influx into native ECs have used several approaches to control V_m including maximal stimulation of muscarinic receptors (e.g. with ACh or methacholine), manipulating extracellular K^+ concentration ($[K^+]_o$), activating or inhibiting K^+ channels, and electrically 'clamping' V_m (Cohen & Jackson, 2005; Dora & Garland, 2013). Complementary experiments have used ECs grown in culture. However, caveats inherent to earlier studies include limited dynamic range of $[Ca^{2+}]_i$ responses, the time course used for controlling V_m, and altered expression of proteins integral to Ca^{2+} signalling. For example, muscarinic receptors can be lost from native ECs when grown in culture (Tracey & Peach, 1992). Cultured ECs may in turn express large-conductance Ca^{2+}-activated K^+ channels (BK_{Ca}) which are otherwise present in SMCs (Sandow & Grayson, 2009). Unlike SK_{Ca}/IK_{Ca}, BK_{Ca} is governed by voltage as well as $[Ca^{2+}]_i$ (Nelson & Quayle, 1995; Jackson, 2005). As determined using intracellular current injection to control V_m throughout the physiological range (∼−80 mV to +10 mV), endothelial 'tubes' freshly isolated from the mouse superior epigastric artery (SEA; a resistance artery supplying abdominal skeletal muscle; *in vivo* diameter, ∼150 μm) lack voltage-gated ion channels and thereby provide a valuable model for addressing whether changes in V_m can modulate Ca^{2+} flux across the plasma membrane. Thus, intracellular injection of negative or positive current enables rigorous evaluation of how changing V_m under prescribed conditions may evoke alterations in $[Ca^{2+}]_i$.

In the present study, we tested the hypothesis that V_m governs $[Ca^{2+}]_i$ of native microvascular ECs. Fura-2 dye was used to monitor $[Ca^{2+}]_i$ while controlling V_m in endothelial tubes freshly isolated from the mouse SEA. The relationship between V_m and $[Ca^{2+}]_i$ was investigated under resting conditions and during half-maximal stimulation with ACh (EC_{50}; 100 nM) to increase (but not maximize) Ca^{2+} permeability of the plasma membrane. Our findings illustrate that during resting conditions, $[Ca^{2+}]_i$ was not affected by changing V_m through a range spanning ∼−80 mV to +10 mV. However, during submaximal stimulation with ACh, $[Ca^{2+}]_i$ increased as V_m hyperpolarized below −40 mV and $[Ca^{2+}]_i$ decreased as V_m depolarized above −40 mV. These effects of altering V_m in the presence of ACh did not occur in the absence of extracellular Ca^{2+} and were attenuated by half in endothelium isolated from TRP vanilloid type 4 channel knockout ($TRPV4^{-/-}$) mice. Thus, V_m can modulate Ca^{2+}

© 2015 The Authors. The Journal of Physiology © 2015 The Physiological Society

influx according to the electrical driving force during submaximal activation of Ca^{2+}-permeable channels in the plasma membrane of microvascular endothelium.

Methods

Animal care and use

All animal care and experimental procedures were approved by the Animal Care and Use Committee of the University of Missouri and performed in accord with the National Research Council's *Guide for the Care and Use of Laboratory Animals* (8th edn, 2011). Mice were housed in an enriched environment maintained on a 12:12 h light–dark cycle at ∼23°C with fresh tap water and standard chow available *ad libitum*. Experiments were performed on male C57BL/6 mice (3–6 months old; $n = 47$) obtained from the National Institute on Aging colonies at Charles River Laboratories (Wilmington, MA, USA). In complementary experiments, male TRPV4$^{-/-}$ mice (C57BL/6 background, 3–6 months old, $n = 5$) bred at the University of Missouri (breeders obtained from GlaxoSmithKline, King of Prussia, PA, USA) were used to investigate the role of TRPV4 (Thorneloe *et al.* 2008). Each mouse was anaesthetized with pentobarbital sodium (60 mg kg^{-1}, intraperitoneal injection) and abdominal fur was removed by shaving. Upon completion of tissue removal, the anaesthetized mouse was killed by exsanguination.

Solutions

All solutions were used at pH 7.4. Control physiological salt solution (PSS) contained the following (in mmol l^{-1}): 2 $CaCl_2$, 140 NaCl, 5 KCl, 1 $MgCl_2$, 10 Hepes, 10 glucose. During microdissection of SEAs, $CaCl_2$ was absent from the PSS to relax SMCs. During dissociation of SMCs to obtain endothelial tubes, PSS contained 0.62 mg ml^{-1} papain (≥6 units), 1.5 mg ml^{-1} collagenase (≥15 units), 1.0 mg ml^{-1} dithioerythritol, 0.1% bovine serum albumin (USB Corp., Cleveland, OH, USA) and 0.1 mmol l^{-1} $CaCl_2$. For experiments with nominally zero $[Ca^{2+}]_o$, $CaCl_2$ was replaced with 2 mM $MgCl_2$ (final $[MgCl_2] = 3$ mM). For experiments with 10 mM $[Ca^{2+}]_o$, NaCl was replaced isosmotically with $CaCl_2$. For experiments with 145 mM $[K^+]_o$, NaCl was replaced on an equimolar basis with KCl. Reagents were obtained from Sigma-Aldrich (St Louis, MO, USA) unless indicated otherwise.

Surgery and microdissection

A ventral midline incision was made through the skin from the sternum to the pubis to expose the abdominal musculature. While viewing through a stereo microscope (SMZ800; Nikon, Tokyo, Japan), fat and connective tissue superficial to the sternum were removed to expose the proximal end of SEAs bilaterally; each was ligated together with its adjacent vein (6-0 silk suture; Ethicon, Somerville, NJ, USA) to maintain blood in the lumen and thereby facilitate visualization during further dissection. The abdominal musculature was removed from the mouse and separated along the *linea alba* and each half was pinned onto transparent silicone rubber (Sylgard 184; Dow Corning, Midland, MI, USA) in control PSS maintained at 4°C. The SEA was dissected free of surrounding tissue from its proximal end to the first branch point (segment length: ∼2 cm) and then cannulated at one end to flush blood from the lumen with PSS. Cannulae were made from borosilicate glass capillaries (G150T-4; Warner Instruments, Hamden, CT, USA) pulled horizontally (P-97; Sutter Instrument Co., Novato, CA, USA), then shaped and heat-polished at one end (tip outer diameter (OD): 50–80 μm) using a custom-built microforge.

Endothelial cell tube isolation and superfusion

Endothelial tubes were prepared as described (Socha & Segal, 2013). Briefly, each SEA was cut into segments 3–5 mm long and incubated in dissociation PSS for 30 min at 37°C. Vessel segments were transferred to a tissue chamber (RC-27N; Warner) containing dissociation PSS at room temperature. To dissociate SMCs, a vessel segment was gently triturated using aspiration and ejection from a micropipette during visual inspection at 200×. Dissociation pipettes (tip internal diameter (ID): ∼80 μm) were prepared from borosilicate glass capillary tubes (1.0 mm OD, 0.58 mm ID; World Precision Instruments (WPI), Sarasota, FL, USA) pulled (P-97; Sutter) and heat-polished at one end. Following dissociation, the tissue chamber containing the endothelial tube was secured to an aluminium platform (width: 14.5 cm, length: 24 cm, thickness: 0.4 cm). A micromanipulator (DT3-100; Siskiyou Corp., Grants Pass, OR, USA) mounted at each end of the platform held a blunt-ended heat-polished micropipette (OD, 60–100 μm) used to position and secure the endothelial tube (width: ∼60 μm, length: ∼1 mm) against the bottom (coverslip) of the tissue chamber. The platform was secured on an inverted microscope (Eclipse TS100, Nikon) mounted on a vibration-isolated table (Technical Manufacturing Corp., Peabody, MA, USA) and superfused at 3–4 ml min^{-1} with control PSS along the axis of the endothelial tube. Throughout experiments, temperature was maintained at 32ºC using an in-line heater (SH-27B; Warner) and heating platform (PH6; Warner) coupled to a temperature controller (TC-344B; Warner). Preparations were stable for the duration of all experiments (1–2 h) under these conditions.

© 2015 The Authors. The Journal of Physiology © 2015 The Physiological Society

Ca^{2+} photometry

Ca^{2+} photometry was performed using an IonOptix system (Milford, MA, USA) as described (Socha *et al.* 2011; Behringer *et al.* 2012). Briefly, prior to loading Fura-2 dye, the preparation was maintained at room temperature for 10 min while autofluorescence was recorded at 510 nm during alternate excitation at 340 and 380 nm (10 Hz). Fura-2 AM dye (5 μM; F14185; Life Technologies, Eugene, OR, USA) was loaded for 20 min followed by a 20 min washout to allow for intracellular de-esterification. Temperature was raised to 32°C during the final 10 min of washout. Autofluorescence (averaged values over 30 s acquisition) during excitation at 340 and 380 nm was subtracted from respective recordings at 510 nm. The photometric window was 140 μm × 50 μm using a 40× objective (Nikon S Fluor; numerical aperture, 0.90) and encompassed ∼50 ECs (Fig. 1). All experiments were performed with 2 mM $[Ca^{2+}]_o$ unless stated otherwise.

To enable approximation of $[Ca^{2+}]_i$ in accord with the Fura-2 ratio, minimum and maximum F_{340}/F_{380} values (R_{min}, 0.43 ± 0.02 and R_{max}, 5.79 ± 0.92, n = 3) were determined in endothelial tubes using a previous protocol with modification (Socha *et al.* 2011). Briefly, endothelial tubes were superfused with PSS containing 0 mM Ca^{2+}, 5 mM EGTA, 1 μM thapsigargin, 1 μM carbonyl cyanide *p*-trifluoromethoxyphenylhydrazone (FCCP) and 3 μM ionomycin for 1 h to deplete intracellular Ca^{2+} (R_{min}), followed by replacement with PSS containing 3 μM ionomycin and 10 mM Ca^{2+} to maximize intracellular Ca^{2+} (R_{max}). Data acquired during respective conditions were also used to calculate the value of β (i.e. F_{min}/F_{max} at 380 nm = 7.40 ± 1.09). The F_{340}/F_{380} (R) values were converted to $[Ca^{2+}]_i$ (in nM) using the equation $[Ca^{2+}]_i = K_d\beta(R - R_{min})/(R_{max} - R)$ (Grynkiewicz *et al.* 1985) assuming an intracellular Fura-2 K_d of 282 nM (Knot & Nelson, 1998).

Intracellular recording and current microinjection

Microelectrodes were pulled (P-97; Sutter) from glass capillary tubes (GC100F-10; Warner) and backfilled with 2 mol l^{-1} KCl (tip resistance, ∼150 MΩ). Using one electrode, current (±0.5 to 5 nA, 20 s pulses) was delivered using an Axoclamp electrometer (2B; Molecular Devices, Sunnyvale, CA, USA) driven by a function generator (CFG253; Tektronix, Beaverton, OR, USA). A second electrode was positioned in an EC located 300 μm downstream (with respect to the direction of PSS superfusion) to record V_m using a second amplifier (IE-210; Warner). An Ag–AgCl pellet placed in effluent PSS served as a reference electrode. Amplifier outputs were connected to an analog-to-digital converter (Digidata 1322A; Molecular Devices) and data were recorded at 1000 Hz on a Dell personal computer using Axoscope 10.1 software (Molecular Devices). Individual cells were penetrated along the midline of the endothelial tube where distance was defined with reference to a calibrated eyepiece reticle while viewing at 400× magnification. Alterations in V_m at the downstream electrode in response to current injected at the upstream electrode verified effective intercellular coupling through gap junctions while 'clamping' V_m in accord with the level of current injection (Behringer & Segal, 2012*b*; Behringer *et al.* 2012, 2013).

Simultaneous Ca^{2+} photometry and electrophysiology

For these experiments, the photometric window (as above) was positioned adjacent to the microelectrode used for recording V_m 300 μm downstream from the site of current microinjection (Fig. 1). Two experimental approaches were used to determine whether (and if so, under what conditions) V_m influenced $[Ca^{2+}]_i$ in accord with its electrochemical driving force across the plasma membrane. In the first approach, NS309 (10 μM) was added to the PSS to open SK_{Ca}/IK_{Ca} maximally and thereby hyperpolarize ECs to approximate the Nernst equilibrium potential for K^+ (E_K; ∼−90 mV) (Strobaek *et al.* 2004; Li *et al.* 2009; Behringer & Segal, 2012*b*). Alternatively, PSS containing 145 mM $[K^+]_o$ was used to clamp V_m in a depolarized state by altering E_K (to ∼0 mV). Respective treatments approximated the boundaries of the physiological range of EC V_m (i.e. ∼−80 to +10 mV) (Ledoux *et al.* 2008) and were administered alone for 2 min then maintained for two additional minutes during exposure to 100 nM ACh. Respective treatments were paired to stimulation with ACh alone (Fig. 2).

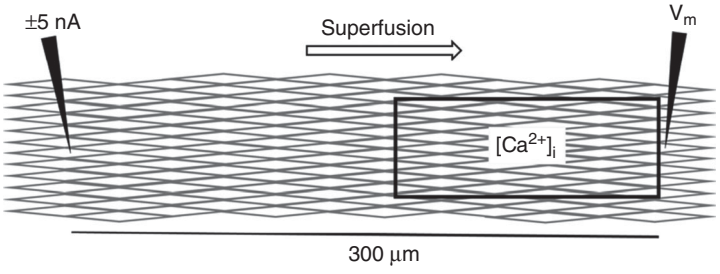

Figure 1. Diagram of simultaneous $[Ca^{2+}]_i$ and V_m measurements in an endothelial tube
A window 140 μm × 50 μm (encompassing ∼50 ECs) monitored $[Ca^{2+}]_i$ using Fura-2 dye photometry. For simultaneous measurements, the window was located adjacent to a microelectrode recording V_m (right) located 300 μm from a microelectrode injecting current (−5 to +5 nA; left) to control (i.e. clamp) V_m at a designated level.

© 2015 The Authors. The Journal of Physiology © 2015 The Physiological Society

In the second approach, defined levels of intracellular current injection were used to clamp V_m incrementally and thereby test how gradations in V_m affected $[Ca^{2+}]_i$ at rest (Fig. 3) and in the presence of 100 nM ACh (Figs 4 and 5). The first series of these experiments evaluated the effect of clamping V_m on $[Ca^{2+}]_i$ before and then during stimulation with ACh. Thus, a designated level of current injection was begun 20 s prior to and maintained throughout 2 min of exposure to 100 nM ACh (see Fig. 4*A*, −3 nA corresponds to V_m of ∼−65 mV; −5 to +5 nA corresponds to V_m ranging from −80 to +10 mV). At ∼30 s following the peak $[Ca^{2+}]_i$ response to ACh (i.e. during the sustained phase of Ca^{2+} influx), current injection was stopped and then resumed in 20 s intervals to evaluate the $[Ca^{2+}]_i$ response to a given level of current injection; data were collected ∼90 s into the stimulation protocol. Following a 3 min washout of ACh to restore resting conditions, this procedure was repeated up to 12 times with respective levels of current injection randomized in magnitude and polarity across experiments. Our previous studies have confirmed that ACh evokes reproducible peak and plateau $[Ca^{2+}]_i$ responses for at least 12 applications repeated in such manner (Behringer *et al.* 2012; Socha *et al.* 2012). The second series of these experiments investigated the effect of changing V_m incrementally from −80 to +10 mV on $[Ca^{2+}]_i$ during the sustained plateau phase of continuous exposure to 100 nM ACh (see Fig. 5*A*). Thus, starting at ∼30 s after the peak $[Ca^{2+}]_i$ response to ACh, each level of current (−5 to +5 nA) was injected for 20 s followed by 20 s of rest, alternating through the entire range of current amplitude and polarity (randomized as above) during ∼10 min of continuous exposure to ACh.

Pharmacology

Throughout experiments, a half-maximal ACh stimulus (100 nM; EC_{50}) (Behringer *et al.* 2012) was used to open Ca^{2+}-permeable ion channels which underlie $[Ca^{2+}]_i$ influx during sustained activation of muscarinic receptors (Busse *et al.* 2002). Our rationale for half-maximal stimulation with ACh was to (1) avoid saturating Ca^{2+} signalling pathways (e.g. as occurs during maximal stimulation with 3 μM ACh; Behringer *et al.* 2012) to thereby allow for dynamic $[Ca^{2+}]_i$ responses (e.g. Ca^{2+} flux through TRP channels) during changes in V_m; and (2) limit the hyperpolarization and current leakage that accompany maximal SK_{Ca}/IK_{Ca} activation during maximal stimulation with ACh (Behringer & Segal, 2012*b*). Other drugs used were NS309 (SK_{Ca}/IK_{Ca} activator), obtained from Tocris Bioscience (Bristol, UK), the TRPV4 agonist GSK1016790A (GSK101) and the TRPV4 antagonist GSK2193874 (GSK219) (Thorneloe *et al.* 2008) obtained from Sigma. As internal controls for the role of TRPV4, complementary experiments were performed using endothelial tubes isolated from SEAs of $TRPV4^{-/-}$ mice in which the expression of TRPV4 was deleted genetically (Thorneloe *et al.* 2008).

Data analyses

Data analyses included (1) fluorescence emission collected at 510 nm and expressed as the ratio during excitation at 340 nm and 380 nm (F_{340}/F_{380}); (2) change in F_{340}/F_{380} ratio ($\Delta F_{340}/F_{380}$) = peak response F_{340}/F_{380} − preceding baseline F_{340}/F_{380}; (3) resting V_m (mV); and (4) change in V_m (ΔV_m) = peak response V_m − preceding baseline V_m. All summary data reflect values averaged over 10 s during stable recordings. Statistical analyses (GraphPad Software, Inc., La Jolla, CA, USA) included linear regression, sigmoidal fits, paired and unpaired Student's *t* tests, and one-way repeated measures analysis of variance with Tukey's *post hoc* comparisons. Differences were accepted as statistically significant with $P < 0.05$. Summary data are presented as means ± SEM. Typically, one endothelial tube was studied per mouse for a given protocol; in some cases a second tube was prepared for study on the same day from the contralateral abdominal muscle (kept in PSS at 4°C) of the same animal. Values of *n* are the number of endothelial tubes studied using a given protocol. With the exception of $TRPV4^{-/-}$ *versus* wild-type preparations, all comparisons are paired (i.e. control *versus* treatment) within a given experimental protocol. Sampling conditions were not altered across preparations and background fluorescence of Fura-2 was collected and subtracted for each experiment.

Results

Our goal was to determine whether V_m can govern endothelial $[Ca^{2+}]_i$ using an experimental strategy that enhanced the open-probability of Ca^{2+}-permeable channels in the plasma membrane and did so without maximizing this signalling pathway. In native microvascular endothelium this condition was evoked via stimulation of muscarinic receptors using a concentration of ACh that approximated the EC_{50} for $[Ca^{2+}]_i$ and V_m (Behringer *et al.* 2012). From the control baseline, 100 nM ACh evoked a rise in F_{340}/F_{380} (Fig. 2*A*). The initial peak reflects intracellular release of Ca^{2+} from the ER, with the sustained plateau attributable to Ca^{2+} influx through the plasma membrane (Cohen & Jackson, 2005; Socha *et al.* 2012). Consistent with original findings (Busse *et al.* 1988), these changes in $[Ca^{2+}]_i$ mirrored the dynamics of V_m (Fig. 2*A*). Indeed, this inverse correspondence between respective signalling events is what led to questioning the relationship(s) between $[Ca^{2+}]_i$ and V_m (Busse *et al.* 2002; Garland *et al.* 2011; Dora & Garland, 2013).

© 2015 The Authors. The Journal of Physiology © 2015 The Physiological Society

Hyperpolarization with NS309 enhances Ca^{2+} influx during stimulation with ACh

We altered V_m by activating SK_{Ca}/IK_{Ca} with NS309 before and during stimulation of muscarinic receptors (Behringer *et al.* 2012). Thus, NS309 (10 μM) hyperpolarized cells from -34 ± 3 mV under control conditions to a stable value of -82 ± 1 mV, yet had no significant effect on F_{340}/F_{380} (Fig. 2*B*). However, the addition of 100 nM ACh evoked a prompt and robust elevation in peak and plateau $[Ca^{2+}]_i$ (Fig. 2*B*) with responses that were ~52% and ~67% greater ($P < 0.05$) than control conditions, respectively (Fig. 2*A*, *B* and *D*, and Table 1).

Depolarization with 145 mM KCl reduces Ca^{2+} influx during stimulation with ACh

To investigate the effect of depolarization on $[Ca^{2+}]_i$, $[K^+]_o$ was raised to 145 mM, lowering V_m from -36 ± 2 mV (rest) to -5 ± 1 mV ($n = 9$). Despite no effect on resting F_{340}/F_{380} or the peak $[Ca^{2+}]_i$ response to 100 nM ACh (Fig. 2*C* and *E*), the plateau F_{340}/F_{380} response was ≈58% lower ($P < 0.05$) than the control response with 5 mM $[K^+]_o$ (Fig. 2*A*, *C* and *E*, and Table 1). The presence of 145 mM $[K^+]_o$ also resulted in a transient secondary rise in $[Ca^{2+}]_i$ at 130 ± 10 s following the initial peak response to ACh (Fig. 2*C*). The amplitude of

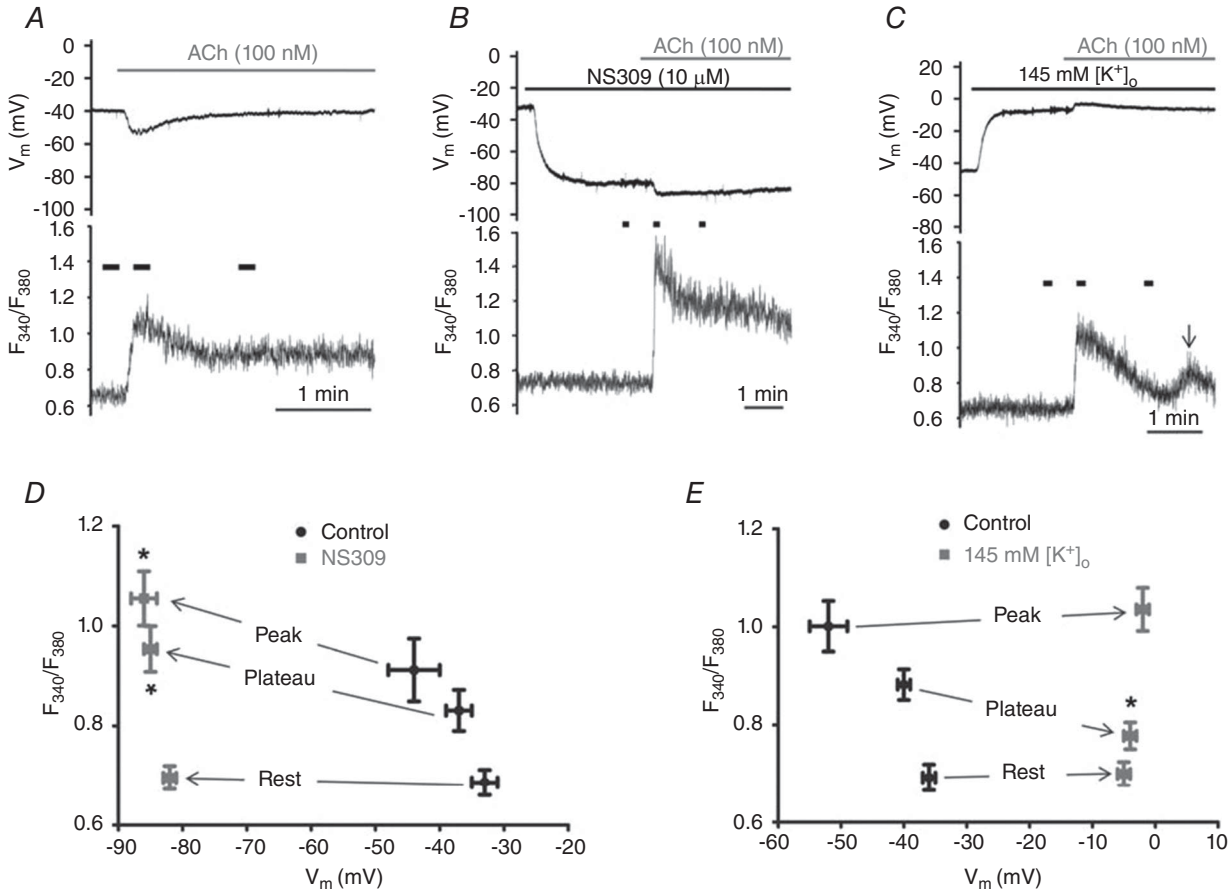

Figure 2. Effects of 10 μm NS309 and 145 mm $[K^+]_o$ on V_m and $[Ca^{2+}]_i$ before and during stimulation with ACh
A, simultaneous V_m (top) and F_{340}/F_{380} (bottom) recordings during 100 nM ACh under control conditions. *B*, as in *A* with 10 μM NS309 pretreatment (2 min) to activate SK_{Ca}/IK_{Ca} preceding ACh. Top: note hyperpolarization to ~80 mV with NS309; ACh increased V_m to ~−85 mV. Bottom: note lack of F_{340}/F_{380} response until ACh is introduced. *C*, as in *A* with 145 mM $[K^+]_o$ pretreatment for 2 min. Depolarization to ~−5 mV had no effect on F_{340}/F_{380} until the addition of ACh. Note diminished F_{340}/F_{380} during plateau phase *versus* control (compare with *A*). Arrow indicates a transient secondary rise in F_{340}/F_{380} ~2 min after initial peak response to ACh. Short horizontal bars above F_{340}/F_{380} traces (bottom panels of *A*–*C*) indicate periods of data acquisition for Rest, Peak and Plateau (90 s after Peak) values, respectively; note difference in time scales. *D*, summary of F_{340}/F_{380} at corresponding V_m before (Rest) and during ACh (Peak and Plateau) for paired experiments before and during NS309 ($n = 10$ endothelial tubes from 10 mice). *E*, as in *D* for paired experiments during ACh alone and during ACh with 145 mM $[K^+]_o$ ($n = 9$ endothelial tubes from 9 mice). *$P < 0.05$, NS309 or 145 mM KCl *versus* respective Control values.

© 2015 The Authors. The Journal of Physiology © 2015 The Physiological Society

this secondary $[Ca^{2+}]_i$ transient was not different from the plateau F_{340}/F_{380} response to 100 nM ACh under control conditions for the same preparations (Table 1).

Intracellular current injection does not alter $[Ca^{2+}]_i$ until stimulation with ACh

Under control conditions, neither hyperpolarizing nor depolarizing current injections (V_m range: -79 ± 2 mV to 10 ± 5 mV) altered resting $[Ca^{2+}]_i$ (Figs. 3*A* and *C*, and 4*B*). Finding that V_m was related linearly to the magnitude and polarity of the injected current (Fig. 3*B*) confirms the lack of voltage-gated ion channels in native ECs (Cohen & Jackson, 2005; Jackson, 2005; Ledoux *et al.* 2008; Behringer *et al.* 2012). The independence of $[Ca^{2+}]_i$ from V_m was maintained throughout the range of current injection (-5 to $+5$ nA; Figs. 3*C* and 4*B*). In contrast, during a given level of hyperpolarization (e.g. -3 nA), addition of 100 nM ACh promptly increased F_{340}/F_{380} (Fig. 4*A*). Further, ensuing current pulses during the plateau phase of the $[Ca^{2+}]_i$ response to ACh changed F_{340}/F_{380} in a manner that increased with the magnitude of hyperpolarization and decreased with the magnitude of depolarization (Fig. 4*C*).

$[Ca^{2+}]_i$ responds bi-directionally to changes in V_m during stimulation with ACh

Despite a large electrochemical gradient for Ca^{2+} entry, the opening of channels permeable to Ca^{2+} is essential for extracellular Ca^{2+} to access the cell interior (Clapham, 2007). In the presence of 100 nM ACh, stepwise current injections (-5 to $+5$ nA) altered V_m from -82 ± 1 mV to 11 ± 3 mV (Fig. 5*A*, top and Fig. 5*B*). As evidenced by concomitant changes in F_{340}/F_{380}, hyperpolarization increased $[Ca^{2+}]_i$ while depolarization decreased $[Ca^{2+}]_i$ (Fig. 5*A*, bottom and Fig. 5*B*). Sigmoid fits to these summary data indicate that V_m at half-maximal F_{340}/F_{380} corresponds to -44 ± 2 mV (Fig. 5*B*). In accord with F_{340}/F_{380} values, estimated $[Ca^{2+}]_i$ concentrations (see Methods) were 104 ± 5 nM at rest and 168 ± 11 nM during the ACh plateau, where injection of -5 nA increased $[Ca^{2+}]_i$ to 246 ± 12 nM and $+5$ nA decreased $[Ca^{2+}]_i$ to 104 ± 5 nM. Thus, while not manifested under control conditions, $[Ca^{2+}]_i$ responds bidirectionally to changing V_m during half-maximal stimulation of muscarinic receptors.

In 30 endothelial tubes from 25 mice, exposure to 100 nM ACh resulted in a plateau $[Ca^{2+}]_i$ response that varied across experiments. Regression analyses of the $\Delta F_{340}/F_{380}$ in response to ACh versus the $\Delta F_{340}/F_{380}$ during current injection revealed no correlation during hyperpolarizing current injections. Thus, while the rise in $[Ca^{2+}]_i$ during hyperpolarization tended to increase with the level of negative current injection, it was independent

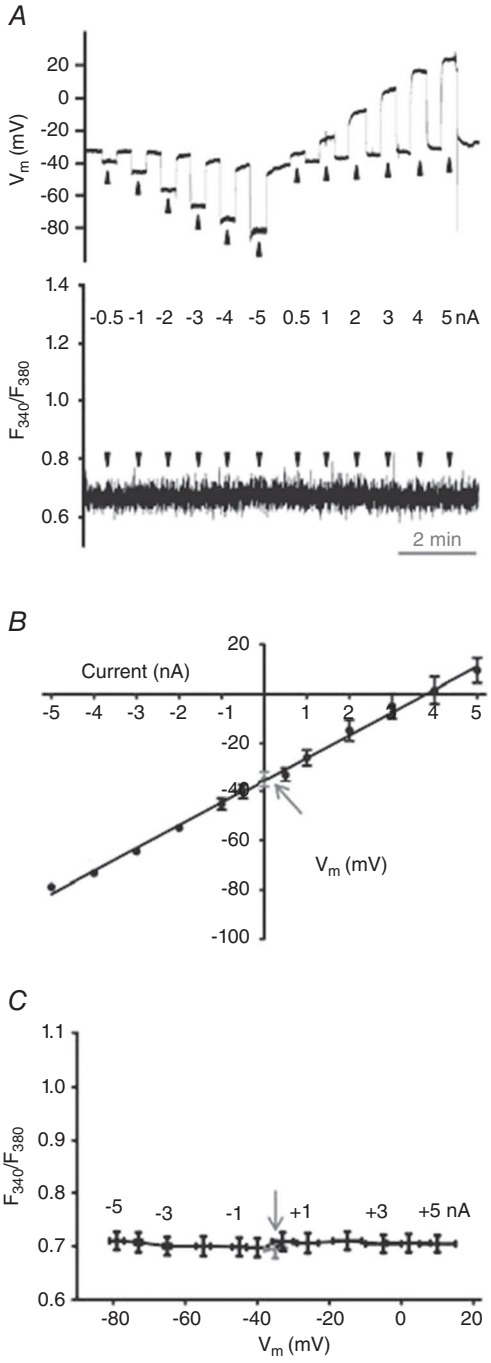

Figure 3. Changing V_m with current injection does not alter resting $[Ca^{2+}]_i$
A, simultaneous V_m (top) and F_{340}/F_{380} (bottom) recordings during control conditions at rest (V_m, -35 ± 3 mV; F_{340}/F_{380}, 0.69 ± 0.02) and during current injection (-5 to $+5$ nA; 20 s pulses at arrowheads). While V_m (top) responded in a stepwise manner F_{340}/F_{380} (bottom) did not change. *B*, linear regression of V_m *versus* injected current ($r^2 = 0.990 \pm 0.002$). *C*, summary data illustrating stability of F_{340}/F_{380} throughout range of V_m during respective levels of current injection (shown near data points for reference). Arrows in *B* and *C* indicate resting V_m and F_{340}/F_{380}, respectively. Summary data binned according to level of current injection for $n = 7$ endothelial tubes from 6 mice.

© 2015 The Authors. The Journal of Physiology © 2015 The Physiological Society

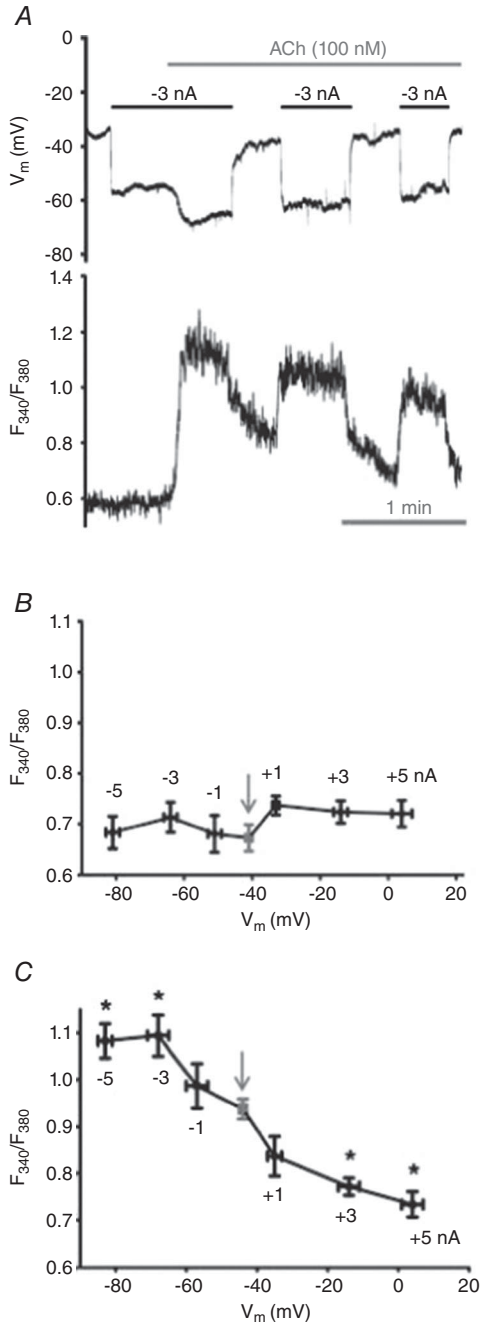

Figure 4. Changing V_m with intracellular current injection alters $[Ca^{2+}]_i$ only during stimulation with ACh
A, simultaneous recordings of V_m (top) and F_{340}/F_{380} (bottom) with −3 nA current pulses before and during 100 nM ACh. Note lack of effect of hyperpolarization on $[Ca^{2+}]_i$ until ACh is introduced. *B*, summary of F_{340}/F_{380} values at designated values of V_m throughout levels of current injection (shown near data points) prior to ACh. Resting F_{340}/F_{380} was not altered from control (arrow) while V_m ranged from −82 ± 2 mV to 4 ± 3 mV. *C*, summary of F_{340}/F_{380} values at designated values of V_m throughout range of current injection during plateau of $[Ca^{2+}]_i$ response to ACh; one current level studied during each ACh stimulation. $^*P < 0.05$, F_{340}/F_{380} during current injection *versus* zero current (arrow; elevated F_{340}/F_{380} versus *B* due to ACh). Summary data in *B* and *C* binned according to level of current injection for $n = 6$–7 endothelial tubes from 6–7 mice.

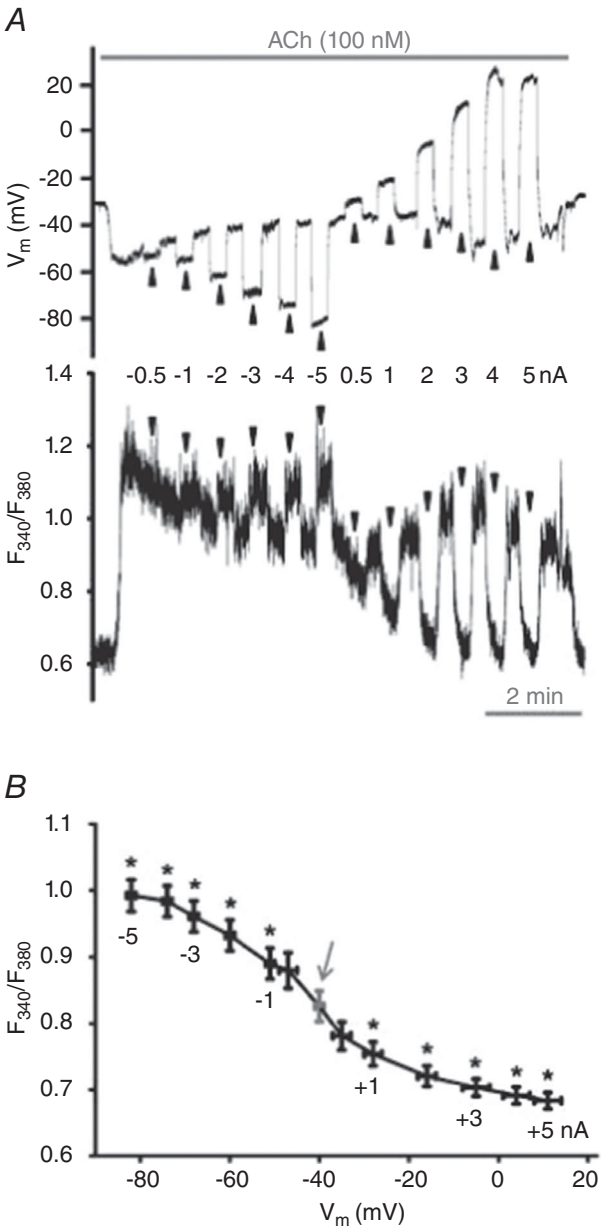

Figure 5. $[Ca^{2+}]_i$ changes with V_m during stimulation with ACh
A, simultaneous V_m (top) and F_{340}/F_{380} (bottom) recordings during current injection (−5 to +5 nA; 20 s pulses at arrowheads) during 100 nM ACh. *B*, summary of F_{340}/F_{380} values for corresponding values of V_m at rest (arrow) and during 100 nM ACh; data binned according to level of current injection (shown near data points). This relationship is sigmoidal ($R^2 = 0.974 \pm 0.005$) with V_m at half-maximal $F_{340}/F_{380} = -44 \pm 2$ mV. Note increase in F_{340}/F_{380} with magnitude of hyperpolarization and decrease in F_{340}/F_{380} (to baseline levels) as V_m approximates 0 mV. Summary data represent $n = 30$ endothelial tubes from 25 mice. $^*P < 0.05$, F_{340}/F_{380} during current injection *versus* F_{340}/F_{380} without current injection (arrow).

© 2015 The Authors. The Journal of Physiology © 2015 The Physiological Society

of the plateau $[Ca^{2+}]_i$ response to ACh (Fig. 6*A*). In contrast, there were significant negative correlations between respective $[Ca^{2+}]_i$ responses during depolarizing current injections (Fig. 6*B*). Thus, reductions in $[Ca^{2+}]_i$ during depolarization increased with the magnitude of the plateau $[Ca^{2+}]_i$ response to ACh, such that +3 nA and +5 nA (corresponding V_m: -5 ± 3 and 11 ± 3 mV) consistently lowered plateau F_{340}/F_{380} to resting levels that preceded stimulation with ACh (see Fig. 5*A*).

$[Ca^{2+}]_i$ responses to changing V_m during stimulation with ACh require extracellular Ca^{2+}

In the absence of extracellular Ca^{2+}, the plateau F_{340}/F_{380} response to ACh was effectively abolished (Table 2). Under these conditions, current injections that altered V_m from -62 ± 4 mV to 13 ± 6 mV had no significant effect on F_{340}/F_{380} (Fig. 7). In the same preparations, including 2 mM $[Ca^{2+}]_o$ resulted in $[Ca^{2+}]_i$ responses consistent with those illustrated in Fig. 5 (Fig. 7*B*). Thus, the rise in $[Ca^{2+}]_i$ during hyperpolarizing current injections reflects Ca^{2+} influx from the extracellular fluid. We then tested whether F_{340}/F_{380} responses to changing V_m in the presence of ACh would be enhanced by elevating $[Ca^{2+}]_o$ to 10 mM. Through the range of −5 nA to +5 nA current injection (with V_m ranging from -90 ± 2 to 2 ± 9 mV), V_m at half-maximal F_{340}/F_{380} shifted to the left from -44 ± 3 mV (with 2 mM $[Ca^{2+}]_o$) to -50 ± 4 mV (with 10 mM $[Ca^{2+}]_o$) and F_{340}/F_{380} was enhanced by ∼7–10% at $V_m \geq -80$ mV ($P < 0.05$; Fig. 8). Further, plateau F_{340}/F_{380} responses to ACh were significantly higher ($P < 0.05$) in the presence of 10 mM $[Ca^{2+}]_o$ compared to control with 2 mM $[Ca^{2+}]_o$ (Table 2). Thus, in the presence of ACh, increasing $[Ca^{2+}]_o$ can augment Ca^{2+} entry during hyperpolarization.

Role of TRPV4 for Ca^{2+} influx during stimulation with ACh

When activated, TRPV4 are integral to Ca^{2+} influx across plasma membranes of vascular endothelium (Zhang *et al.* 2009; Sonkusare *et al.* 2012; Qian *et al.* 2014). We therefore tested the role of TRPV4 in mediating Ca^{2+} entry in response to changing V_m using genetic and pharmacological approaches. Under resting conditions, F_{340}/F_{380} and V_m of endothelial tubes from TRPV4$^{-/-}$ mice (0.72 ± 0.03 and −34 ± 3 mV, respectively; $n = 8$) were not significantly different from those of wild-type C57BL/6 mice (0.68 ± 0.01 and −37 ± 1 mV, respectively; $n = 30$; Table 3). During stimulation with 100 nM ACh, injecting −5 nA to +5 nA in TRPV4$^{-/-}$ altered V_m from -79 ± 5 mV to 15 ± 7 mV and $[Ca^{2+}]_i$ increased with $V_m \geq$ ∼−65 mV (Fig. 9*A* and *B*). When compared to C57BL/6 mice, F_{340}/F_{380} responses in endothelial tubes

Table 1. Effects of hyperpolarization (10 μm NS309) and depolarization (145 mm $[K^+]_o$ on $[Ca^{2+}]_i$ and V_m responses to ACh

	F_{340}/F_{380}					V_m (mV)					
Condition	Rest	Peak	Peak Δ	Plateau	Plateau Δ	Rest	Peak	Peak Δ	Plateau	Plateau Δ	*n*
Control	0.69 ± 0.03	0.91 ± 0.06	0.23 ± 0.07	0.83 ± 0.04	0.15 ± 0.04	−33 ± 2	−44 ± 4	−11 ± 4	−37 ± 2	−4 ± 1	10
NS309 (10 μM)	0.70 ± 0.03	1.06 ± 0.05*	0.35 ± 0.05*	0.95 ± 0.05*	0.25 ± 0.04*	−82 ± 1*	−86 ± 2*	−4 ± 1*	−85 ± 1*	−4 ± 1	10
Control	0.69 ± 0.03	1.00 ± 0.05	0.31 ± 0.06	0.88 ± 0.06	0.19 ± 0.04	−36 ± 1	−52 ± 3	−16 ± 4	−40 ± 1	−4 ± 1	9
145 mM $[K^+]_o$	0.70 ± 0.02	1.04 ± 0.04	0.34 ± 0.05	0.78 ± 0.03*	0.08 ± 0.01*	−5 ± 1*	−2 ± 1*	3 ± 1*	−4 ± 1*	2 ± 1*	9

Summary of values for Resting, Peak and Plateau phases for $[Ca^{2+}]_i$ (F_{340}/F_{380}, $\Delta F_{340}/F_{380}$) and membrane potential (V_m, ΔV_m) of endothelial tubes during stimulation with 100 nM ACh (see Fig. 2). $[Ca^{2+}]_o$ was 2 mM for all experiments. ACh was present under all conditions except 'Rest'.
*$P < 0.05$, treatment *versus* paired Control.

© 2015 The Authors. The Journal of Physiology © 2015 The Physiological Society

from TRPV4$^{-/-}$ mice were reduced by ∼50% at $V_m \geq -60$ mV (Fig. 9*C*).

When applied to endothelial tubes of wild-type C57BL/6 mice, the TRPV4 antagonist GSK219 (1 μM) tended to reduce F_{340}/F_{380} values and resting V_m but these effects were not statistically significant (Table 3). However GSK219 suppressed the $[Ca^{2+}]_i$ response to hyperpolarizing current injection during stimulation with 100 nM ACh. Thus, −3 nA increased Plateau F_{340}/F_{380} to 1.09 ± 0.03 under control conditions and this response was reduced to 0.94 ± 0.04 ($P < 0.05$, $n = 6$) in the presence of 1 μM GSK219 despite no difference in hyperpolarization (V_m = −72 ± 4 mV and −76 ± 5 mV, respectively). Application of the TRPV4 agonist GSK101 (1–10 nM) to endothelial tubes of C57BL/6 mice produced hyperpolarization (rest: −38 ± 5 mV, GSK101: −53 ± 4 mV) and increased F_{340}/F_{380} from 0.70 ± 0.03 (rest) to 0.84 ± 0.03 (GSK101; $n = 4$, $P < 0.05$); however $[Ca^{2+}]_i$ did not

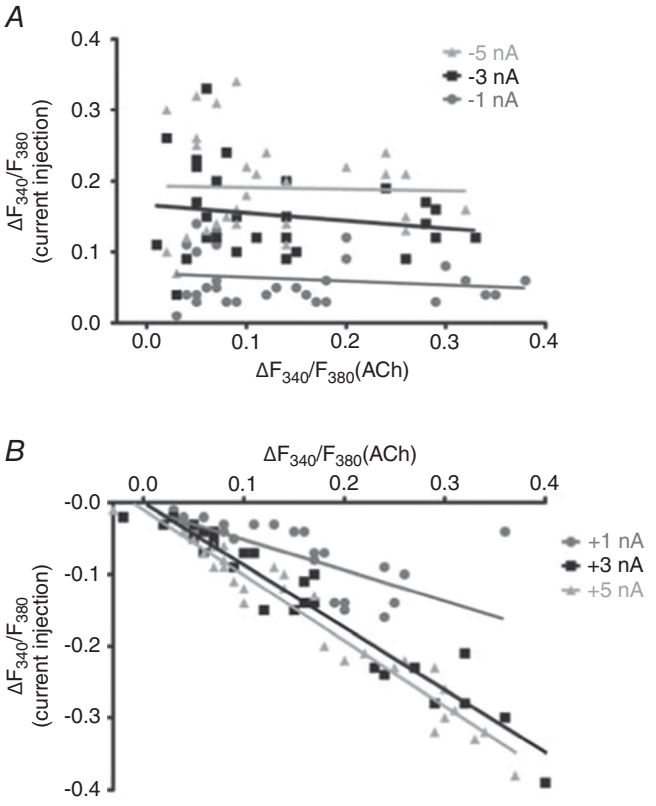

Figure 6. Plateau $[Ca^{2+}]_i$ responses to ACh correlate with $[Ca^{2+}]_i$ responses to depolarization
A, scatter plot illustrating magnitude of $\Delta F_{340}/F_{380}$ during negative current injections of −1, −3 and −5 nA during the plateau $\Delta F_{340}/F_{380}$ response to 100 nM ACh (*Y*-axis) *versus* the plateau $\Delta F_{340}/F_{380}$ response (from resting baseline) to 100 nM ACh (*X*-axis). Note lack of correlation ($R^2 < 0.035$). *B*, as in *A* during positive current injections of +1, +3 and +5 nA. Note negative correlations between the decreased $[Ca^{2+}]_i$ during depolarization and the plateau $[Ca^{2+}]_i$ response to ACh ($R^2 > 0.55$). Individual data points correspond to summary data in Fig. 5*B*.

Table 2. Effect of extracellular Ca^{2+} on $[Ca^{2+}]_i$ and V_m responses to ACh

	F_{340}/F_{380}					V_m (mV)				
Condition	Rest	Peak	Peak Δ	Plateau	Plateau Δ	Rest	Peak	Peak Δ	Plateau	Plateau Δ	*n*
Control	0.72 ± 0.01	0.96 ± 0.07	0.24 ± 0.07	0.82 ± 0.03	0.11 ± 0.03	−39 ± 4	−49 ± 5	−10 ± 4	−42 ± 4	−3 ± 1	8
0 $[Ca^{2+}]_o$	0.69 ± 0.02	0.81 ± 0.05*	0.12 ± 0.04*	0.71 ± 0.02*	0.03 ± 0.01*	−25 ± 2*	−31 ± 2*	−6 ± 2	−24 ± 2*	−1 ± 1*	8
Control	0.68 ± 0.01	0.86 ± 0.04	0.18 ± 0.04	0.79 ± 0.03	0.10 ± 0.03	−36 ± 3	−41 ± 3	−5 ± 1	−38 ± 3	−2 ± 1	10
10 mM $[Ca^{2+}]_o$	0.71 ± 0.02	1.12 ± 0.04*	0.41 ± 0.04*	0.93 ± 0.02*	0.22 ± 0.03*	−52 ± 4*	−63 ± 3*	−11 ± 2*	−57 ± 4*	−5 ± 2	10

Summary of values for Resting, Peak and Plateau phases for $[Ca^{2+}]_i$ (F_{340}/F_{380}, $\Delta F_{340}/F_{380}$) and membrane potential (V_m, ΔV_m) of endothelial tubes during stimulation with 100 nM ACh when $[Ca^{2+}]_o$ was nominally 0 (Ca^{2+}-free PSS) or elevated to 10 mM and compared to respective Controls with $[Ca^{2+}]_o$ = 2 mM. ACh was present under all conditions except 'Rest'. Note that removal of $[Ca^{2+}]_o$ was associated with depolarization while elevating $[Ca^{2+}]_o$ to 10 mM was associated with hyperpolarization. *$P < 0.05$, treatment *versus* paired Control.

© 2015 The Authors. The Journal of Physiology © 2015 The Physiological Society

increase further during hyperpolarizing current injection (for −3 nA: $\Delta F_{340}/F_{380}$: 0.01 ± 0.01, ΔV_m:−23 ± 5 mV). Thus, in the presence of ACh, TRPV4 activation in wild-type endothelium contributes to Ca^{2+} influx during hyperpolarization. While genetic deletion of TRPV4 or its pharmacological inhibition with GSK219 impaired the effect of hyperpolarization on promoting Ca^{2+} entry during ACh stimulation, pharmacological activation of TRPV4 with GSK101 did not increase $[Ca^{2+}]_i$ during hyperpolarization.

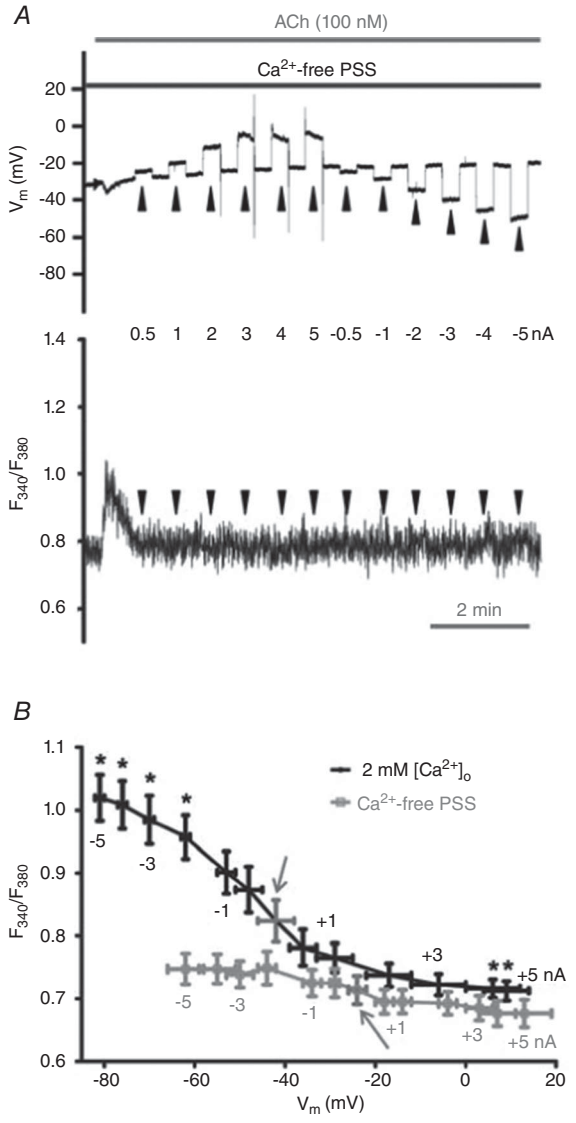

Figure 7. $[Ca^{2+}]_i$ responses to changing V_m during stimulation with ACh require extracellular Ca^{2+}
A, simultaneous V_m (top) and F_{340}/F_{380} (bottom) recordings during current injection (−5 to +5 nA; 20 s pulses at arrowheads) during 100 nM ACh in Ca^{2+}-free PSS. Note absence of sustained elevation (i.e. plateau phase) in $[Ca^{2+}]_i$ response. *B*, overlay of summary data for F_{340}/F_{380} values at corresponding levels of V_m (binned according to level of current injection) during 100 nM ACh with 2 mM $[Ca^{2+}]_o$ and with Ca^{2+}-free PSS. Arrows indicate V_m and F_{340}/F_{380} under respective conditions with zero current. Summary data are paired experiments for $n = 8$ endothelial tubes from 8 mice. $^*P < 0.05$, F_{340}/F_{380} during current injection *versus* F_{340}/F_{380} with zero current.

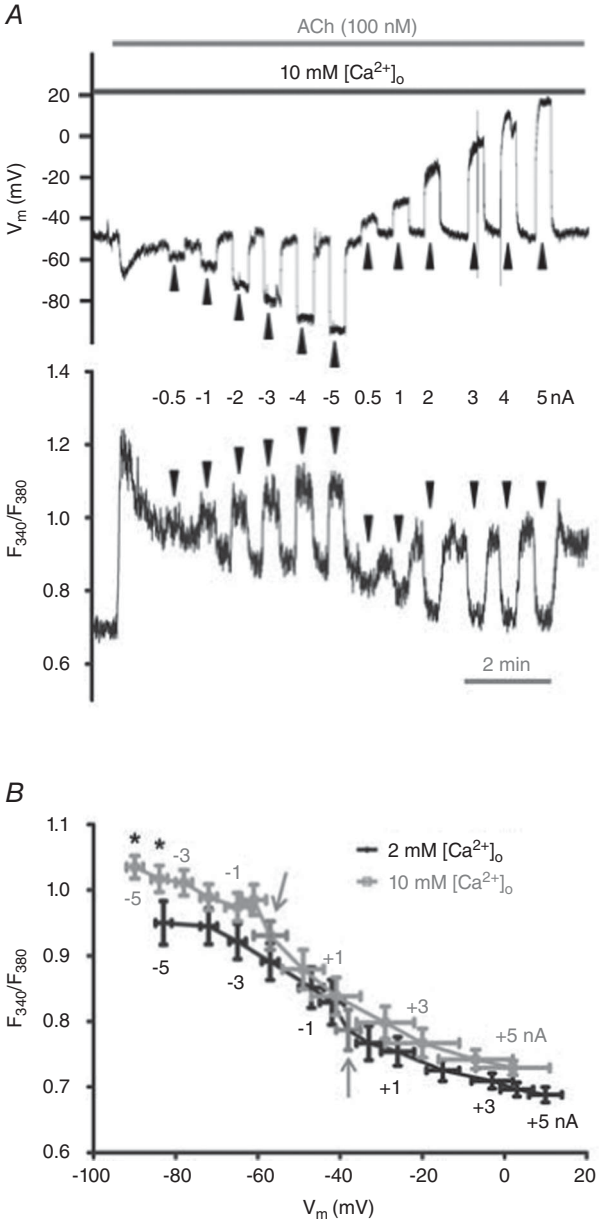

Figure 8. Increasing $[Ca^{2+}]_o$ increases $[Ca^{2+}]_i$ with maximal hyperpolarization during stimulation with ACh
A, simultaneous V_m (top) and F_{340}/F_{380} (bottom) recordings during current injection (−5 to +5 nA; 20 s pulses at arrowheads) during 100 nM ACh; $[Ca^{2+}]_o$ = 10 mM. *B*, overlay of summary data for F_{340}/F_{380} values at corresponding levels of V_m (binned according to level of current injection). Arrows indicate V_m and F_{340}/F_{380} during plateau response to ACh with zero current. Summary data are paired experiments for $n = 10$ endothelial tubes from 10 mice. $^*P < 0.05$, F_{340}/F_{380} during 10 mM $[Ca^{2+}]_o$ *versus* 2 mM $[Ca^{2+}]_o$.

© 2015 The Authors. The Journal of Physiology © 2015 The Physiological Society

Table 3. Effect of TRPV4 on $[Ca^{2+}]_i$ and V_m responses to ACh

	(F_{340}/F_{380})					V_m (mV)				
Condition	Rest	Peak	Peak Δ	Plateau	Plateau Δ	Rest	Peak	Peak Δ	Plateau	Plateau Δ	*n*
Wild-type	0.68 ± 0.01	0.97 ± 0.03	0.28 ± 0.03	0.83 ± 0.02	0.14 ± 0.02	−37 ± 1	−50 ± 2	−13 ± 2	−40 ± 1	−3 ± 1	30
TRPV4$^{-/-}$	0.72 ± 0.03	0.80 ± 0.04*	0.08 ± 0.02*	0.76 ± 0.04	0.04 ± 0.01*	−34 ± 3	−40 ± 3*	−6 ± 1*	−37 ± 2	−2 ± 1	8
Wild-type Control	0.73 ± 0.02	1.18 ± 0.06	0.45 ± 0.06	0.98 ± 0.04	0.25 ± 0.04	−41 ± 4	−62 ± 5	−21 ± 5	−51 ± 4	−11 ± 3	6
Wild-type GSK219	0.70 ± 0.03	1.12 ± 0.03	0.42 ± 0.03	0.88 ± 0.04	0.19 ± 0.02	−33 ± 3	−63 ± 4	−30 ± 6	−44 ± 6	−11 ± 4	6

Summary of values for Rest, Peak and Plateau phases for $[Ca^{2+}]_i$ (F_{340}/F_{380}, $\Delta F_{340}/F_{380}$) and membrane potential (V_m, ΔV_m) of endothelial tubes during stimulation with 100 nM ACh in endothelial tubes from wild-type (C57BL/6) *versus* TRPV4$^{-/-}$ mice and from wild-type (C57BL/6) before (Control) and during exposure to the TRPV4 antagonist GSK2193874 (GSK219; 1 μM). $[Ca^{2+}]_o$ = 2 mM under all conditions. ACh was present under all conditions except 'Rest'.
*$P < 0.05$, TRPV4$^{-/-}$ *versus* wild-type.

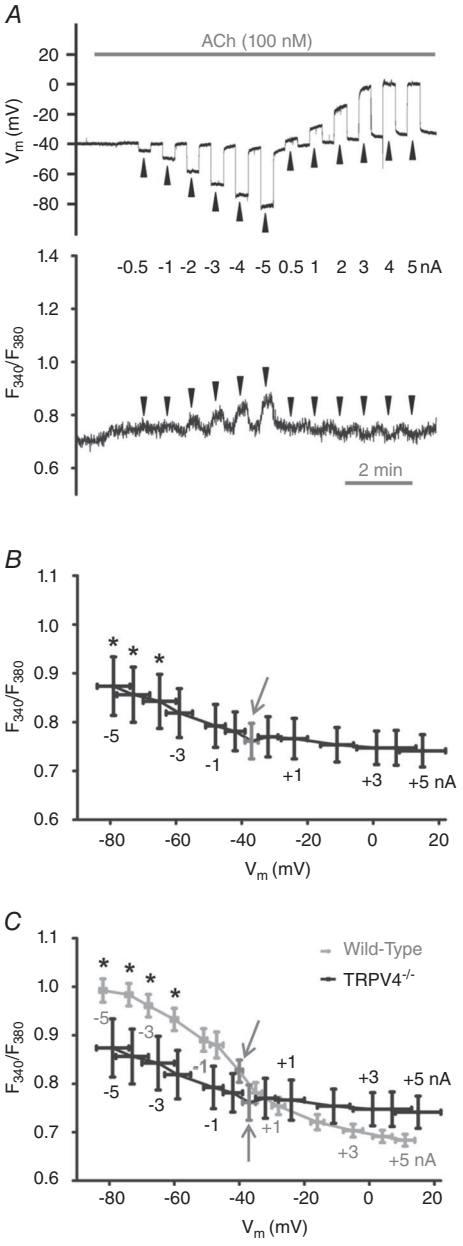

Figure 9. Lack of TRPV4 expression attenuates Ca^{2+} influx with hyperpolarization during stimulation with ACh
A, simultaneous V_m (top) and F_{340}/F_{380} (bottom) recordings in the presence of 100 nM ACh during current injection (alternating 20 s pulses at arrowheads) in endothelial tube from a TRPV4$^{-/-}$ mouse. *B*, summary data for F_{340}/F_{380} at corresponding V_m (binned according to level of current injection) during 100 nM ACh in endothelial tubes from TRPV4$^{-/-}$ mice. *$P < 0.05$, F_{340}/F_{380} during current injection *versus* no current injection (arrow). Data represent 8 endothelial tubes from 5 TRPV4$^{-/-}$ mice. *C*, overlay of summary data from *B* with data from wild-type (C57BL/6) mice (from Fig. 5*B*) at corresponding levels of V_m and current injection (all experiments with $[Ca^{2+}]_o$ = 2 mM). Arrows indicate values with zero current. *$P < 0.05$, F_{340}/F_{380} of wild-type *versus* TRPV4$^{-/-}$ at given level of current injection.

© 2015 The Authors. The Journal of Physiology © 2015 The Physiological Society

Discussion

The relationship between V_m and EC $[Ca^{2+}]_i$ is central to the regulation of tissue blood flow with Ca^{2+} serving as an integral second messenger during endothelium-dependent vasodilatation (Busse *et al.* 2002; Ledoux *et al.* 2006; Bagher & Segal, 2011; Garland *et al.* 2011). Whether hyperpolarization promotes Ca^{2+} entry in vascular ECs has remained controversial for more than 25 years. The driving force for Ca^{2+} into the cell is manifested by a ∼20,000-fold concentration gradient from the extracellular to the intracellular compartments complemented by electronegativity of the cell interior (Clapham, 2007). However, cell membranes must be permeable to Ca^{2+} for influx to occur. In this study, we questioned whether changes in V_m alone or in conjunction with activation of muscarinic receptors could alter $[Ca^{2+}]_i$ of intact endothelium freshly isolated from resistance arteries of mouse skeletal muscle. We reasoned that if Ca^{2+}-permeable channels were inactive at rest, then changing V_m should be ineffective in altering resting $[Ca^{2+}]_i$. Complementary approaches altered V_m under resting conditions and while Ca^{2+}-permeable channels were opened submaximally with ACh, i.e. during the plateau phase of signalling dominated by Ca^{2+} influx. Our principal findings demonstrate that, under resting conditions, $[Ca^{2+}]_i$ was unaffected when V_m was shifted through a range of ∼90 mV (i.e. from −80 mV to +10 mV). In striking contrast, in the presence of 100 nM ACh, $[Ca^{2+}]_i$ increased in response to hyperpolarization and decreased in response to depolarization from a resting V_m of ∼−40 mV. This effect of changing V_m on $[Ca^{2+}]_i$ was lost following removal of extracellular Ca^{2+} and was attenuated by half in endothelium of TRPV4$^{-/-}$ mice. Thus, V_m modulates Ca^{2+} entry during submaximal activation of Ca^{2+}-permeable ion channels in the plasma membrane of native microvascular endothelium.

Experimental considerations

Complexity of Ca^{2+} signalling. A potentially confounding variable in studies of intact vessels is that ECs can be coupled directly (via myoendothelial gap junctions) to SMCs, which do express voltage activated ion channels (Jackson, 2005; Ledoux *et al.* 2006) and may affect EC $[Ca^{2+}]_i$ indirectly via myoendothelial coupling (Sonkusare *et al.* 2012; Tran *et al.* 2012; Dora & Garland, 2013). Thus, to resolve the relationship between V_m and Ca^{2+} entry strictly in accord with electrochemical driving force requires that (1) only the endothelium is present; (2) the experimental approach does not activate voltage-gated ion channels; (3) V_m is altered independent of $[Ca^{2+}]_i$ while both variables are evaluated simultaneously; and (4) experimental manipulations are of sufficient intensity and duration to evoke definitive responses without saturating (and thereby masking) the variables under investigation. In light of previous efforts to resolve the effect of V_m on $[Ca^{2+}]_i$ (see citations in Dora & Garland, 2013), the present experiments endeavoured to ensure that respective criteria were satisfied to the extent possible.

The physiological integration between Ca^{2+} release from the ER and its influx through the plasma membrane can complicate experimental approaches attempting to resolve endothelial Ca^{2+} dynamics following muscarinic receptor stimulation. For example, preventing release of Ca^{2+} from the ER precludes the key physiological stimulus for Ca^{2+} influx (Bishara *et al.* 2002). Thus, our approach for investigating how Ca^{2+} influx may be governed by V_m during submaximal stimulation of muscarinic receptors included removal of extracellular Ca^{2+}, raising $[Ca^{2+}]_o$ to 10 mM and determining the effect of eliminating an integral Ca^{2+}-permeable membrane channel by studying endothelial tubes of TRPV4$^{-/-}$ mice as well as pharmacological inhibition of TRPV4 in endothelial tubes of wild-type mice.

Calcium photometry. Our evaluation of $[Ca^{2+}]_i$ relied on photometry and reflects 'global' levels as recorded simultaneously from ∼50 ECs contained within the window used for detecting intracellular fluorescence (Fig. 1). This approach is consistent with methods employed by previous investigators evaluating the relationship between V_m and $[Ca^{2+}]_i$ (Busse *et al.* 1988; Cohen & Jackson, 2005; McSherry *et al.* 2005). In contrast, confocal imaging has been used to detect Ca^{2+} signalling events (i.e. 'sparklets') localized to single Ca^{2+} channels (e.g. TRPV4) in the plasma membrane of individual ECs within myoendothelial projections that contact SMCs (Bagher *et al.* 2012; Sonkusare *et al.* 2012; Tran *et al.* 2012; Sonkusare *et al.* 2014). However, during the isolation of endothelial tubes, removal of SMCs obviates myoendothelial projections. An advantage of Ca^{2+} photometry is the ability to acquire data from the same cells throughout protocols lasting 10–15 min (e.g. Figs 3, 5 and 7–9). Such prolonged recording is not possible with confocal imaging due to photobleaching of dye indicators. Thus, Fura-2 photometry concomitant with intracellular recording enables resolution of whether, and under what conditions, 'global' $[Ca^{2+}]_i$ of native microvascular endothelium can be governed in response to altering V_m. Our use of 100 nM ACh in the present experiments was to approximate half-maximal (i.e. EC_{50}) levels of Ca^{2+} signalling and to limit the loss of charge during current injection to be able to control V_m (Behringer & Segal, 2012*b*). Using confocal imaging of the same preparations studied here, 100 nM ACh elicited spatially restricted Ca^{2+} events in single cells (i.e. Ca^{2+} 'puffs'), whereas 1 μM ACh evoked the propagation of Ca^{2+} waves within and between neighbouring ECs (Socha *et al.* 2012). A question for imaging studies in the future is whether imposing

© 2015 The Authors. The Journal of Physiology © 2015 The Physiological Society

hyperpolarization during submaximal stimulation with ACh can elevate Ca^{2+} signalling from discrete intracellular events to the generation and propagation of Ca^{2+} waves.

Intracellular recording. The V_m of ECs was clamped for defined intervals (e.g. 20 s) by injecting negative or positive current through an intracellular microelectrode. As these cells are coupled electrically through gap junctions, the change in V_m is conducted from cell to cell, decaying with distance from the site of current injection (Behringer & Segal, 2012*b*). Monitoring V_m adjacent to the site of Ca^{2+} photometry (Fig. 1) enabled the relationship between endothelial V_m and $[Ca^{2+}]_i$ to be evaluated remotely from the site of current injection while confirming the key physiological property of electrical conduction. Thus V_m was controlled through a physiological range in accord with the magnitude and polarity of injected current. Nevertheless, current can 'leak' out of cells during ion channel activation as shown for SK_{Ca}/IK_{Ca} (Behringer & Segal, 2012*b*). Thus the ability to control V_m using current injection and thereby determine the effect of V_m on $[Ca^{2+}]_i$ is compromised with interventions that activate ion channels to a sufficient extent, e.g. during maximal stimulation with 3 μM ACh (Behringer & Segal, 2012*b*). We therefore used an EC_{50} ACh stimulus to evaluate how V_m affected Ca^{2+} entry while avoiding saturation of this signalling pathway.

Present and previous approaches

In the present experiments, multiple approaches were used to investigate the effect of V_m on $[Ca^{2+}]_i$ with ACh used as a tool to activate Ca^{2+}-permeable channels half-maximally. Near-maximal hyperpolarization was achieved by opening SK_{Ca}/IK_{Ca} directly with 10 μM NS309 (Behringer & Segal, 2012*b*). Alternatively, maximal depolarization was imposed using 145 mM $[K^+]_o$ to shift the Nernst potential for K^+ to zero versus ~ -90 mV with 5 mM $[K^+]_o$. To explore the relationship between V_m and $[Ca^{2+}]_i$ with greater resolution, incremental changes in V_m were imposed using graded levels of current injected through an intracellular microelectrode.

Under resting conditions, neither chemical nor electrical interventions altered $[Ca^{2+}]_i$ despite V_m ranging from -80 to $+10$ mV (Figs 2–5). Endothelium of the mouse SEA lacks voltage-gated ion channel activity as demonstrated by strictly linear voltage responses through this range in V_m during current injection (Fig. 3; Behringer & Segal, 2012*b*; Behringer *et al.* 2012). Such behaviour is consistent with findings from native endothelium in several vascular beds including skeletal muscle, and mesenteric and cerebral arteries of mice, rats and hamsters (Cohen & Jackson, 2005; Jackson, 2005; Ledoux *et al.* 2008). In contrast, studies of cultured ECs have detected a progressive decrease in resting $[Ca^{2+}]_i$ from a V_m of -100 mV to $+60$ mV (Cannell & Sage, 1989; Laskey *et al.* 1990; Sharma & Davis, 1995), suggesting the presence of voltage-sensitive ion channels. The expression of membrane proteins can be altered when ECs are grown in culture. Thus, the acquisition of large-conductance Ca^{2+} activated K^+ channels (Sandow & Grayson, 2009) may impart voltage sensitivity while the loss of muscarinic receptors (Tracey & Peach, 1992) has necessitated the use of alternative agonists (e.g. bradykinin) to initiate Ca^{2+} signalling, thereby complicating comparisons to experiments performed on native endothelium stimulated with ACh.

Near-maximal hyperpolarization with NS309 amplified the $[Ca^{2+}]_i$ response to ACh (Fig. 2*A*, *B* and *D*) while maximal depolarization with 145 mM $[K^+]_o$ reduced the plateau phase of the $[Ca^{2+}]_i$ response to ACh (Fig. 2*C* and *E*). In the presence of 100 nM ACh, -5 nA hyperpolarized the endothelium and enhanced plateau $[Ca^{2+}]_i$ similar to what was achieved using 10 μM NS309 (compare Fig. 2*D* with Figs 4*C* and 5*B*). Conversely, injection of $+3$ nA depolarized the endothelium and decreased the plateau $[Ca^{2+}]_i$ response to ACh similar to the action of 145 mM $[K^+]_o$ (compare Fig. 2*E* with Figs 4*C* and 5*B*). In contrast, studies of endothelium freshly isolated from arterioles of the hamster cremaster muscle found that the plateau $[Ca^{2+}]_i$ responses to methacholine (1 μM) was unaffected by depolarization with 145 mM $[K^+]_o$ (Cohen & Jackson, 2005) while experiments performed on intact rat mesenteric arteries found that the $[Ca^{2+}]_i$ response to 0.3 μM ACh was unaffected by depolarization with 35 mM KCl (McSherry *et al.* 2005). These latter findings are consistent with studies of native endothelium from several laboratories indicating that changes in endothelial $[Ca^{2+}]_i$ were independent of changes in V_m (Marrelli *et al.* 2003; Takano *et al.* 2004; Cohen & Jackson, 2005; McSherry *et al.* 2005; Qian *et al.* 2014). It is possible that the level of Ca^{2+} influx stimulated by muscarinic receptor activation (and Ca^{2+} depletion from the ER) superseded any effect of hyperpolarization on Ca^{2+} influx. Nevertheless, several studies of cultured ECs have supported a role for V_m in modulating Ca^{2+} influx during stimulation of G protein-coupled receptors. For example, hyperpolarization and depolarization using voltage clamp, manipulation of $[K^+]_o$ and/or altering K^+ channel activity were found to increase and decrease $[Ca^{2+}]_i$, respectively during stimulation with ACh, bradykinin or histamine (Cannell & Sage, 1989; Laskey *et al.* 1990; Luckhoff & Busse, 1990; Sharma & Davis, 1995; Li *et al.* 1999).

An unexpected yet consistent finding was a transient secondary rise of F_{340}/F_{380} values during depolarization with 145 mM $[K^+]_o$ in the presence of 100 nM ACh. The

© 2015 The Authors. The Journal of Physiology © 2015 The Physiological Society

amplitude of this secondary response was not different from the plateau F_{340}/F_{380} values of paired controls with 100 nM ACh alone (Table 1; compare Fig. 2*C* bottom trace at arrow to Fig. 2*A* bottom trace during plateau]. While the mechanism underlying this secondary rise in $[Ca^{2+}]_i$ is unknown, it may entail a delayed decrease in the function of the Na^+/Ca^{2+} exchanger as a consequence of a low $[Na^+]_o$ due to equimolar replacement with K^+ during exposure to 145 mM $[K^+]_o$. Thus the time window used for data acquisition during the plateau phase of Ca^{2+} signalling may be critical for resolving the effects of depolarization using elevated $[K^+]_o$.

New insights into V_m and Ca^{2+} signalling in endothelium of resistance vessels

Using dual intracellular microelectrodes to investigate the effect of controlling V_m on the regulation of $[Ca^{2+}]_i$, the present findings illustrate that the relationship between V_m and $[Ca^{2+}]_i$ during stimulation with 100 nM ACh is sigmoidal in nature (Fig. 5*B*) and requires extracellular Ca^{2+} (Fig. 7). Values for F_{340}/F_{380} effectively plateaued with $V_m > \sim -60$ mV or $< \sim -25$ mV (Fig. 5*B*) and the effect of V_m on F_{340}/F_{380} when $[Ca^{2+}]_o$ was raised to 10 mM was significantly different from control ($[Ca^{2+}]_o = 2$ mM) only with $V_m > -80$ mV) (Fig. 8). Thus, with a resting V_m of ~ -30 to -40 mV (Welsh & Segal, 1998; Emerson & Segal, 2000; Wolfle *et al.* 2011; Behringer & Segal, 2012*b*), the V_m range of -25 to -60 mV appears to have the greatest physiological relevance to the regulation of $[Ca^{2+}]_i$ by V_m during submaximal activation of Ca^{2+}-permeable channels in the plasma membrane of ECs. Indeed, maximal dilatation of feed arteries and arterioles can be evoked with 10–15 mV of hyperpolarization (Emerson & Segal, 2000; Wolfle *et al.* 2011). Thus, a sigmoidal relationship between endothelial V_m and $[Ca^{2+}]_i$ signalling that is centred near resting V_m is consistent with the physiological regulation of blood flow via endothelium-dependent hyperpolarization. In turn, finding that the plateau elevation in $[Ca^{2+}]_i$ can be reversed by depolarizing the cell interior to < -10 mV (Figs. 4*C* and 5*B*) suggests that sufficient hyperpolarization is required for increases in $[Ca^{2+}]_i$ to be governed by V_m. An unexpected finding is that, while the ability to increase $[Ca^{2+}]_i$ during incremental levels of hyperpolarization did not correlate with the magnitude of the $[Ca^{2+}]_i$ response to ACh (Fig. 6*A*), decreases in $[Ca^{2+}]_i$ during incremental depolarization were correlated with the magnitude of the plateau $[Ca^{2+}]_i$ response to ACh (Fig. 6*B*). These results suggest that the ability of depolarization to restore $[Ca^{2+}]_i$ to resting levels reflects the marked ability of ECs to sequester or extrude cytosolic Ca^{2+} during a reduced electrical gradient for Ca^{2+} influx.

Role of TRPV4

Recent studies have demonstrated an integral role of TRPV4 for promoting endothelial Ca^{2+} influx and dilatation of resistance arteries via activation of SK_{Ca}/IK_{Ca} (i.e. endothelium-dependent hyperpolarization) (Zhang *et al.* 2009; Sonkusare *et al.* 2012; Qian *et al.* 2014). In intact resistance arteries, pharmacological blockade and/or genetic deletion of TRPV4 were shown to reduce Ca^{2+} signalling and vasodilatation in response to ACh by ≥70% (Zhang *et al.* 2009; Sonkusare *et al.* 2012; Qian *et al.* 2014). Our findings using endothelial tubes from $TRPV4^{-/-}$ mice indicate that TRPV4 may account for nearly half of the capacity to increase $[Ca^{2+}]_i$ in response to $V_m \geq -60$ mV during half-maximal stimulation with ACh (Fig. 9) and that this effect can be mimicked in the endothelium of wild-type mice using pharmacological inhibition with GSK219. The remaining $[Ca^{2+}]_i$ response under these conditions may reflect Ca^{2+}-permeable channels comprising other TRP channels (e.g. TRPC1,3,4,5,6/TRPV1,3/TRPA1; Yue *et al.* 2015) that assemble in a homomeric or heteromeric fashion (Cheng *et al.* 2007; Earley *et al.* 2007; Ma *et al.* 2010). The contribution of other TRP channels may also explain why the activation of TRPV4 alone with GSK101 increased baseline $[Ca^{2+}]_i$ yet had no further effect during current injection. Taken together, previous and current findings indicate that TRPV4, at least in part, contributes to both Ca^{2+}-induced hyperpolarization and hyperpolarization-induced Ca^{2+} entry underlying endothelium-dependent vasodilatation in the regulation of tissue blood flow.

Physiological significance of hyperpolarization-induced Ca^{2+} entry

The use of hyperpolarizing agents (e.g. K^+ channel activators) may help to alleviate decrements in vasodilatation and thereby restore tissue perfusion during cardiovascular disease (Wulff & Kohler, 2013). Indeed, pharmacological activation of SK_{Ca}/IK_{Ca} with SKA-31 has been found to produce EC hyperpolarization and a reduction in arterial blood pressure (Damkjaer *et al.* 2012). Such actions have been found to ameliorate complications of hypertension (Radtke *et al.* 2013) and to promote coronary blood flow in diabetic hearts (Mishra *et al.* 2014). The mechanism underlying such benefits of SK_{Ca}/IK_{Ca} activation may reflect hyperpolarization-induced Ca^{2+} entry to amplify SK_{Ca}/IK_{Ca} activity and/or NO production and can be evoked via submaximal stimulation of muscarinic receptors with ACh. However, there is a balance between the strength of initiating hyperpolarization at sites of stimulation and the ability to conduct the electrical signal along the vessel wall through gap junctions coupling

© 2015 The Authors. The Journal of Physiology © 2015 The Physiological Society

ECs to each other and to surrounding SMCs. Activating SK_{Ca}/IK_{Ca} to the extent where V_m exceeds −60 mV results in current leakage that restricts the spread of hyperpolarization by more than half (Behringer & Segal, 2012*b*; Behringer *et al.* 2013). Under such conditions, charge loss through electrically leaky membranes impairs the ability of conducted vasodilatation to coordinate blood flow regulation among branches of vascular resistance networks (Behringer & Segal, 2012*a*). Thus, invoking hyperpolarization-induced Ca^{2+} entry (and activation of SK_{Ca}/IK_{Ca} in general) should be viewed with caution, as increasing SK_{Ca}/IK_{Ca} activation may be beneficial up to the point at which vasodilator signals fail to initiate and/or spread effectively. In light of current understanding with respect to how hyperpolarization is initiated and conducted to promote vasodilatation (Emerson & Segal, 2000; Wolfle *et al.* 2011; Behringer & Segal, 2012*b*; Behringer *et al.* 2013), we suggest that excessive activation of SK_{Ca}/IK_{Ca} may supersede effective physiological regulation of tissue perfusion.

Summary and perspective

An integral component of endothelial function in the resistance vasculature entails Ca^{2+} and electrical signalling to govern vessel diameter and tissue perfusion. The increase in EC $[Ca^{2+}]_i$ leads to SMC relaxation and vasodilatation through production of vasodilator autacoids (e.g. NO) and the initiation of hyperpolarization (via SK_{Ca}/IK_{Ca} activation) that can spread from cell to cell along and among the branches of resistance networks to coordinate blood flow distribution and magnitude according to local and global metabolic demand. The present findings illustrate that V_m can modulate Ca^{2+} entry into the ECs (e.g. through TRPV4) during submaximal stimulation of muscarinic receptors. However this signalling pathway is effectively closed under resting conditions and Ca^{2+} entry can be saturated during maximal receptor stimulation, likely to be a consequence of depleting Ca^{2+} stores within the endoplasmic reticulum. Nevertheless, when Ca^{2+} entry is submaximal, EC $[Ca^{2+}]_i$ increases with hyperpolarization and decreases with depolarization through a physiological range when initiated from resting V_m. The interplay between V_m and $[Ca^{2+}]_i$ signalling revealed here in native microvascular endothelium helps to resolve earlier controversy regarding the role of V_m in governing $[Ca^{2+}]_i$ and provides new insight into the physiological regulation of vascular resistance. The ability to modulate $[Ca^{2+}]_i$ by changing V_m (e.g. through activation or inhibition of specific ion channels) may be employed judiciously to adjust irregularities in the behaviour of resistance vessels that control blood pressure and tissue perfusion during cardiovascular disease.

References

Bagher P, Beleznai T, Kansui Y, Mitchell R, Garland CJ & Dora KA (2012). Low intravascular pressure activates endothelial cell TRPV4 channels, local Ca^{2+} events, and IK_{Ca} channels, reducing arteriolar tone. *Proc Natl Acad Sci USA* **109**, 18174–18179.

Bagher P & Segal SS (2011). Regulation of blood flow in the microcirculation: role of conducted vasodilation. *Acta Physiol (Oxf)* **202**, 271–284.

Behringer EJ & Segal SS (2012*a*). Spreading the signal for vasodilatation: implications for skeletal muscle blood flow control and the effects of ageing. *J Physiol* **590**, 6277–6284.

Behringer EJ & Segal SS (2012*b*). Tuning electrical conduction along endothelial tubes of resistance arteries through Ca^{2+}-activated K^+ channels. *Circ Res* **110**, 1311–1321.

Behringer EJ, Shaw RL, Westcott EB, Socha MJ & Segal SS (2013). Aging impairs electrical conduction along endothelium of resistance arteries through enhanced Ca^{2+}-activated K^+ channel activation. *Arterioscler Thromb Vasc Biol* **33**, 1892–1901.

Behringer EJ, Socha MJ, Polo-Parada L & Segal SS (2012). Electrical conduction along endothelial cell tubes from mouse feed arteries: Confounding actions of glycyrrhetinic acid derivatives. *Br J Pharmacol* **166**, 774–787.

Bishara NB, Murphy TV & Hill MA (2002). Capacitative Ca^{2+} entry in vascular endothelial cells is mediated via pathways sensitive to 2 aminoethoxydiphenyl borate and xestospongin C. *Br J Pharmacol* **135**, 119–128.

Busse R, Edwards G, Feletou M, Fleming I, Vanhoutte PM & Weston AH (2002). EDHF: bringing the concepts together. *Trends Pharmacol Sci* **23**, 374–380.

Busse R, Fichtner H, Luckhoff A & Kohlhardt M (1988). Hyperpolarization and increased free calcium in acetylcholine-stimulated endothelial cells. *Am J Physiol Heart Circ Physiol* **255**, H965–H969.

Busse R & Mulsch A (1990). Calcium-dependent nitric oxide synthesis in endothelial cytosol is mediated by calmodulin. *FEBS Lett* **265**, 133–136.

Cannell MB & Sage SO (1989). Bradykinin-evoked changes in cytosolic calcium and membrane currents in cultured bovine pulmonary artery endothelial cells. *J Physiol* **419**, 555–568.

Cheng W, Yang F, Takanishi CL & Zheng J (2007). Thermosensitive TRPV channel subunits coassemble into heteromeric channels with intermediate conductance and gating properties. *J Gen Physiol* **129**, 191–207.

Clapham DE (2007). Calcium signaling. *Cell* **131**, 1047–1058.

Cohen KD & Jackson WF (2005). Membrane hyperpolarization is not required for sustained muscarinic agonist-induced increases in intracellular Ca^{2+} in arteriolar endothelial cells. *Microcirculation* **12**, 169–182.

Damkjaer M, Nielsen G, Bodendiek S, Staehr M, Gramsbergen JB, deWit C, Jensen BL, Simonsen U, Bie P, Wulff H & Kohler R (2012). Pharmacological activation of $K_{Ca}3.1/K_{Ca}2.3$ channels produces endothelial hyperpolarization and lowers blood pressure in conscious dogs. *Br J Pharmacol* **165**, 223–234.

Dora KA & Garland CJ (2013). Linking hyperpolarization to endothelial cell calcium events in arterioles. *Microcirculation* **20**, 248–256.

© 2015 The Authors. The Journal of Physiology © 2015 The Physiological Society

Earley S, Reading S & Brayden JE (2007). Functional significance of transient receptor potential channels in vascular function. In *TRP Ion Channel Function in Sensory Transduction and Cellular Signaling Cascades*, ed. Liedtke WB & Heller S, pp. 361–376. CRC Press, Boca Raton.

Emerson GG & Segal SS (2000). Endothelial cell pathway for conduction of hyperpolarization and vasodilation along hamster feed artery. *Circ Res* **86**, 94–100.

Garland CJ, Hiley CR & Dora KA (2011). EDHF: spreading the influence of the endothelium. *Br J Pharmacol* **164**, 839–852.

Grynkiewicz G, Poenie M & Tsien RY (1985). A new generation of Ca^{2+} indicators with greatly improved fluorescence properties. *J Biol Chem* **260**, 3440–3450.

Himmel HM, Whorton AR & Strauss HC (1993). Intracellular calcium, currents, and stimulus-response coupling in endothelial cells. *Hypertension* **21**, 112–127.

Jackson WF (2005). Potassium channels in the peripheral microcirculation. *Microcirculation* **12**, 113–127.

Knot HJ & Nelson MT (1998). Regulation of arterial diameter and wall $[Ca^{2+}]$ in cerebral arteries of rat by membrane potential and intravascular pressure. *J Physiol* **508**, 199–209.

Laskey RE, Adams DJ, Johns A, Rubanyi GM & vanBreemen C (1990). Membrane potential and Na^{+}-K^{+} pump activity modulate resting and bradykinin-stimulated changes in cytosolic free calcium in cultured endothelial cells from bovine atria. *J Biol Chem* **265**, 2613–2619.

Ledoux J, Bonev AD & Nelson MT (2008). Ca^{2+}-activated K^{+} channels in murine endothelial cells: block by intracellular calcium and magnesium. *J Gen Physiol* **131**, 125–135.

Ledoux J, Werner ME, Brayden JE & Nelson MT (2006). Calcium-activated potassium channels and the regulation of vascular tone. *Physiology (Bethesda)* **21**, 69–78.

Li L, Bressler B, Prameya R, Dorovini-Zis K & VanBreemen C (1999). Agonist-stimulated calcium entry in primary cultures of human cerebral microvascular endothelial cells. *Microvasc Res* **57**, 211–226.

Li W, Halling DB, Hall AW & Aldrich RW (2009). EF hands at the N-lobe of calmodulin are required for both SK channel gating and stable SK-calmodulin interaction. *J Gen Physiol* **134**, 281–293.

Luckhoff A & Busse R (1990). Activators of potassium channels enhance calcium influx into endothelial cells as a consequence of potassium currents. *Naunyn Schmiedebergs Arch Pharmacol* **342**, 94–99.

Ma X, Cao J, Luo J, Nilius B, Huang Y, Ambudkar IS & Yao X (2010). Depletion of intracellular Ca^{2+} stores stimulates the translocation of vanilloid transient receptor potential 4-c1 heteromeric channels to the plasma membrane. *Arterioscler Thromb Vasc Biol* **30**, 2249–2255.

Marrelli SP, Eckmann MS & Hunte MS (2003). Role of endothelial intermediate conductance K_{Ca} channels in cerebral EDHF-mediated dilations. *Am J Physiol Heart Circ Physiol* **285**, H1590–H1599.

McSherry IN, Spitaler MM, Takano H & Dora KA (2005). Endothelial cell Ca^{2+} increases are independent of membrane potential in pressurized rat mesenteric arteries. *Cell Calcium* **38**, 23–33.

Mishra RC, Wulff H, Cole WC & Braun AP (2014). A pharmacologic activator of endothelial K_{Ca} channels enhances coronary flow in the hearts of type 2 diabetic rats. *J Mol Cell Cardiol* **72**, 364–373.

Nelson MT & Quayle JM (1995). Physiological roles and properties of potassium channels in arterial smooth muscle. *Am J Physiol Cell Physiol* **268**, C799–C822.

Qian X, Francis M, Kohler R, Solodushko V, Lin M & Taylor MS (2014). Positive feedback regulation of agonist-stimulated endothelial Ca^{2+} dynamics by $K_{Ca}3.1$ channels in mouse mesenteric arteries. *Arterioscler Thromb Vasc Biol* **34**, 127–135.

Radtke J, Schmidt K, Wulff H, Kohler R & deWit C (2013). Activation of $K_{Ca}3.1$ by SKA-31 induces arteriolar dilatation and lowers blood pressure in normo- and hypertensive connexin40-deficient mice. *Br J Pharmacol* **170**, 293–303.

Ruhle B & Trebak M (2013). Emerging roles for native Orai Ca^{2+} channels in cardiovascular disease. *Curr Top Membr* **71**, 209–235.

Sandow SL & Grayson TH (2009). Limits of isolation and culture: intact vascular endothelium and BK_{Ca}. *Am J Physiol Heart Circ Physiol* **297**, H1–H7.

Sharma NR & Davis MJ (1995). Substance P-induced calcium entry in endothelial cells is secondary to depletion of intracellular stores. *Am J Physiol Heart Circ Physiol* **268**, H962–H973.

Socha MJ, Domeier TL, Behringer EJ & Segal SS (2012). Coordination of intercellular Ca^{2+} signaling in endothelial cell tubes of mouse resistance arteries. *Microcirculation* **19**, 757–770.

Socha MJ, Hakim CH, Jackson WF & Segal SS (2011). Temperature effects on morphological integrity and Ca^{2+} signaling in freshly isolated murine feed artery endothelial cell tubes. *Am J Physiol Heart Circ Physiol* **301**, H773–H783.

Socha MJ & Segal SS (2013). Isolation of microvascular endothelial tubes from mouse resistance arteries. *J Vis Exp* **81**, e50759.

Sonkusare SK, Bonev AD, Ledoux J, Liedtke W, Kotlikoff MI, Heppner TJ, Hill-Eubanks DC & Nelson MT (2012). Elementary Ca^{2+} signals through endothelial TRPV4 channels regulate vascular function. *Science* **336**, 597–601.

Sonkusare SK, Dalsgaard T, Bonev AD, Hill-Eubanks DC, Kotlikoff MI, Scott JD, Santana LF & Nelson MT (2014). AKAP150-dependent cooperative TRPV4 channel gating is central to endothelium-dependent vasodilation and is disrupted in hypertension. *Sci Signal* **7**, ra66.

Strobaek D, Teuber L, Jorgensen TD, Ahring PK, Kjaer K, Hansen RS, Olesen SP, Christophersen P & Skaaning-Jensen B (2004). Activation of human IK and SK Ca^{2+}-activated K^{+} channels by NS309 (6,7-dichloro-1*H*-indole-2,3-dione 3-oxime). *Biochim Biophys Acta* **1665**, 1–5.

Takano H, Dora KA, Spitaler MM & Garland CJ (2004). Spreading dilatation in rat mesenteric arteries associated with calcium-independent endothelial cell hyperpolarization. *J Physiol* **556**, 887–903.

© 2015 The Authors. The Journal of Physiology © 2015 The Physiological Society

Thorneloe KS, Sulpizio AC, Lin Z, Figueroa DJ, Clouse AK, McCafferty GP, Chendrimada TP, Lashinger ES, Gordon E, Evans L, Misajet BA, Demarini DJ, Nation JH, Casillas LN, Marquis RW, Votta BJ, Sheardown SA, Xu X, Brooks DP, Laping NJ & Westfall TD (2008). *N*-((1*S*)-1-{[4-((2*S*)-2-{[(2,4-Dichlorophenyl)sulfonyl]amino}-3-hydroxypropanoyl)-1-piperazinyl]carbonyl}-3-methylbutyl)-1-benzothiophene-2-carboxamide (GSK1016790A), a novel and potent transient receptor potential vanilloid 4 channel agonist induces urinary bladder contraction and hyperactivity: Part I. *J Pharmacol Exp Ther* **326**, 432–442.

Tracey WR & Peach MJ (1992). Differential muscarinic receptor mRNA expression by freshly isolated and cultured bovine aortic endothelial cells. *Circ Res* **70**, 234–240.

Tran CH, Taylor MS, Plane F, Nagaraja S, Tsoukias NM, Solodushko V, Vigmond EJ, Furstenhaupt T, Brigdan M & Welsh DG (2012). Endothelial Ca^{2+} wavelets and the induction of myoendothelial feedback. *Am J Physiol Cell Physiol* **302**, C1226–C1242.

Welsh DG & Segal SS (1998). Endothelial and smooth muscle cell conduction in arterioles controlling blood flow. *Am J Physiol Heart Circ Physiol* **274**, H178–H186.

Wolfle SE, Chaston DJ, Goto K, Sandow SL, Edwards FR & Hill CE (2011). Non-linear relationship between hyperpolarisation and relaxation enables long distance propagation of vasodilatation. *J Physiol* **589**, 2607–2623.

Wulff H & Kohler R (2013). Endothelial small-conductance and intermediate-conductance KCa channels: an update on their pharmacology and usefulness as cardiovascular targets. *J Cardiovasc Pharmacol* **61**, 102–112.

Yue Z, Xie J, Yu AS, Stock J, Du J & Yue L (2015). Role of TRP channels in the cardiovascular system. *Am J Physiol Heart Circ Physiol* **308**, H157–H182.

Zhang DX, Mendoza SA, Bubolz AH, Mizuno A, Ge ZD, Li R, Warltier DC, Suzuki M & Gutterman DD (2009). Transient receptor potential vanilloid type 4-deficient mice exhibit impaired endothelium-dependent relaxation induced by acetylcholine in vitro and in vivo. *Hypertension* **53**, 532–538.

Additional information

Competing interests

The authors have declared no competing interests.

Author contributions

E.J.B. designed and performed experiments in the laboratory of S.S.S., analysed and interpreted the data, drafted the manuscript and prepared the figures. S.S.S. contributed to experimental design and the interpretation and presentation of data, and edited the manuscript. Both authors approved the final version of the manuscript for publication.

Funding

This research was supported by National Institutes of Health grant R37-HL041026 to S.S.S. E.J.B. was supported by NIH grants 5T32-AR048523 and 1K99-AG047198. The content of this article is solely the responsibility of the authors and does not necessarily represent the official views of the National Institutes of Health.

Acknowledgements

Dr William F. Jackson provided helpful comments in the early stages of these experiments.

Author's present address

E. J. Behringer: Loma Linda University, School of Medicine, Basic Sciences: Division of Pharmacology, Risley Hall, 11041 Campus Street, Loma Linda, CA 92354, USA.

© 2015 The Authors. The Journal of Physiology © 2015 The Physiological Society